Iranian Polymer Journal (2020) 29:433–443
https://doi.org/10.1007/s13726-020-00808-6

ORIGINAL RESEARCH

Phosphorus- and silicon-containing amino curing agent for epoxy resin

Ajinkya Satdive[1] · Siddhesh Mestry[1] · Pavan Borse[1] · Shashank Mhaske[1]

Received: 29 November 2019 / Accepted: 10 March 2020 / Published online: 23 March 2020

Abstract

Current research work focuses on the synthesis of phosphorus- and silicon-containing amine curing agent (PSA) for epoxy resins. PSA was synthesized using phenyl phosphonic dichloride and ethylenediamine as raw materials and further modification with 3-glycidoxypropyltrimethoxysilane. NMR, FTIR and amine value analysis were performed for the structure confirmation of the obtained product and intermediate. PSA was taken in different molar ratios for the crosslinking with epoxy resin before which the sol–gel technique was performed onto the product for self-crosslinking of the methoxy groups. The obtained formulations were applied onto the mild steel panels and cured in an oven. The thermal and mechanical properties of cured epoxy resins were analyzed by TGA, DSC, impact resistance, pencil hardness and flexibility. The thermal and mechanical properties were increased along with the heat resistance index temperature (T_{HRI}) toward the loading of PSA into the coating formulations. The flame retardant properties were also checked and found to be increased with respect to the increasing concentration of PSA because of the synergistic effect of P and Si atoms. The formulation with the highest amount of PSA showed the highest LOI as 29 with self-extinguishing behavior in the UL-94 test.

Keywords Amine curing agent · Flame retardant · Phosphorus · Silicon · Sol–gel

Introduction

Epoxy resins are one of the important classes of the polymeric materials having various applications such as aerospace composites, printed circuit boards, metal can coatings, adhesives and automotive primers. These resins have a huge demand in consumer markets because of various outstanding properties such as excellent chemical, moisture and corrosion resistance, remarkable mechanical strength and toughness, adhesion to many substrates and good insulation properties. However, epoxy resins possess poor flame retardancy due to their weak oxidation resistance [1] which is forcing researchers to develop the epoxy resins with improved flame retardancy without compromising their fundamental properties and stringent environmental regulations [2]. Many times, epoxies prove to be futile when applications require high flame retardancy as they are highly flammable. However, this property can be improved either by physical dispersion of flame retardants (FRs) into the polymer matrix [3] or by chemical bonding of FRs to the polymer backbone [4].

Halogen-containing moieties are widely used as FR materials, but these compounds emit hazardous and corrosive gases in the form of hydrogen halides during the mechanism of action which is harmful to the environment and human health. Hence, the development of halogen-free FRs is one of the major concerns in academic as well as in industrial research [5]. Phosphorus-containing FRs have received much attention because of being less toxic to the environment than halogenated FRs and their simple mechanism of action [6]. Halogenated organophosphorus compounds are the most reactive phosphorus-containing FRs as they react easily with the compounds having active protons such as amines, alcohols, phenols and carboxylic acids [7]. These compounds give better flame retardancy than halogenated compounds because of their condensed phase mechanism in which they form char barrier between the flame and the substrate [8].

Electronic supplementary material The online version of this article (https://doi.org/10.1007/s13726-020-00808-6) contains supplementary material, which is available to authorized users.

✉ Shashank Mhaske
stmhaske@gmail.com; st.mhaske@ictmumbai.edu.in

[1] Department of Polymer and Surface Engineering, Institute of Chemical Technology, Mumbai 400019, India

Numerous studies have shown that the compounds containing silicon can increase flame retardancy, mechanical properties and oxidation resistance, to correlate with the reduced flammability of the material [9, 10]. The phosphorus-containing compounds act through char formation with some additional gas-phase flame retardancy, while silicon-containing compounds help in increasing the char yield. Moreover, the combination of silicon-containing compounds with diamine curing agents may lead to higher char yield and increased flame retardancy [11]. Ménard et al. [12] successfully synthesized epoxy monomer and phosphorus-containing flame retardant by using phloroglucinol, while Liu et al. synthesized phosphorus-containing epoxy resin for FR application. Lin et al. [13] synthesized bis-biphenyloxy (4-hydroxy) phenyl phosphine oxide which showed an increase in char yield due to the incorporation of phenylphosphonic dichloridex. Furthermore, Agrawal et al. [1] have synthesized phosphorus- and silicon-containing FR curing agents to study their effects on the thermal properties of epoxy resins.

The present work reports the synthesis of novel phosphorus- and silicon-based curing agent for epoxy resins which can be used as a reactive FR moiety. The final product was used along with the commercial polyamide in different proportions for curing the commercial epoxy. The obtained coating films were studied for various thermal, mechanical and FR properties.

Experimental

Materials

Phenylphosphonic dichloride (PPDC) and ethylenediamine (EDA) were purchased from Sigma-Aldrich. Triethylamine (TEA), acetone, hydrochloric acid (HCl) and ethyl acetate (EA) were purchased from SD Fine Chem. Ltd., Mumbai, India. 3-Glycidoxypropyltrimethoxysilane (GPTMS) was purchased from Alfa Aesar Ltd., Mumbai (India). Epoxy resin was supplied by Grand Polycoats Pvt., Ltd., India (epoxy equivalent weight, EEW 184), while polyether amine D230 (amine hydrogen equivalent weight, AHEW 60) from BASF Ltd., India, was used as a commercial hardener. All chemicals were of LR grade and were used without any treatment. The mild steel panels were used for coating application.

Synthesis of phosphorus-containing amine (PA)

EDA (1.68 g, 0.028 mol), TEA (2.93 g, 0.028 mol) as a catalyst and acetone as a solvent were charged into a four-necked round bottom flask equipped with a mechanical stirrer, a thermometer and a reflux condenser. The reaction was carried out in an ice bath under the inert atmosphere. PPDC (2.72 g, 0.014 mol) was added dropwise maintaining the temperature below 5 °C, and the reaction mixture was stirred continuously for 24 h at room temperature after the complete addition of PPDC. The reaction product was then washed with water to remove TEA, and the final product was extracted using EA, followed by the evaporation of EA under vacuum.

Reaction of PA with GPTMS

In the second step (Fig. 1), PA (3.63 g, 0.015 mol) and GPTMS (2.14 g, 0.030 mol) were added into a four-necked round bottom flask equipped with a thermometer, mechanical stirrer and a reflux condenser. The reaction was carried out for 5 h at 60–65 °C with acetone as a solvent. After the completion of the reaction, the solvent was evaporated under vacuum to obtain the final product (PSA). The reaction was monitored using amine value.

Preparation of FR coating

The required quantity of the obtained compound was calculated based on the concept of curing chemistry of the epoxy coating in accordance with replaceable protons available in the structure and subjected to the sol–gel technique. The desired quantity of the product was subjected to the hydrolysis and self-condensation by stirring in pH 2 solution at 50 °C for 2 h, followed by drying in an oven at 70 °C for water evaporation and facilitating condensation of methoxy groups. The obtained gel-like sticky mass was then incorporated into the commercial epoxy resin in various concentrations along with the commercial polyamide forming the coatings (EPSA), and the concentrations of the ingredients used are shown in Table 1. The concentration of PSA was varied from 10 to 40%, and the formulation was applied over mild steel panels by a bar applicator. The panels were cured in an oven at 120 °C for 2 h, and the cured coatings were characterized by various mechanical and thermal properties (Fig. 2).

Characterization

The amine value of PA and PSA was determined by volumetric titration method according to ASTM D2074-07. The known quantity of sample was dissolved in isopropyl alcohol, and 2–3 drops of bromocresol green indicator were added and titrated against 0.5 N HCl solution. Equation 1 is used to calculate the amine values:

$$\text{Amine value} = \frac{\text{Burette Reading} \times \text{Normality of HCl} \times 56.1}{\text{Weight of the sample in grams}}. \quad (1)$$

To determine the gel content, the cured films were carefully peeled off from the Teflon sheet. The known weight

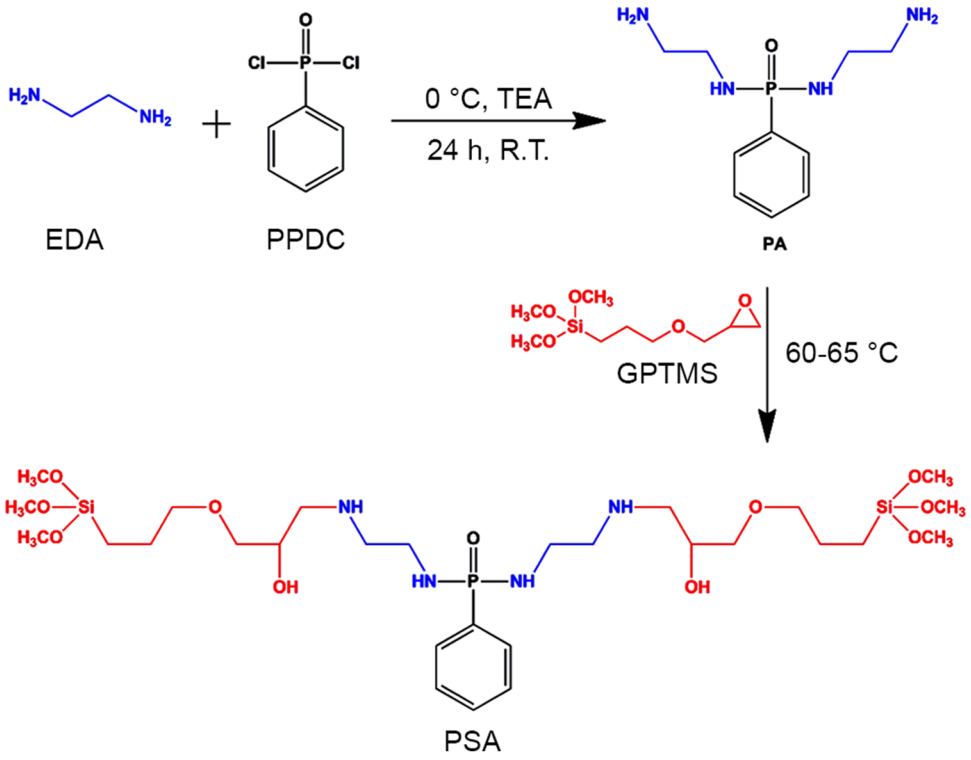

Fig. 1 Schematic diagram showing the synthesis of PA and PSA

Table 1 Formulations of EPSA coatings

Sample	Commercial polyamide (%)	PSA (%)
0EPSA	100	0
10EPSA	90	10
20EPSA	80	20
30EPSA	70	30
40EPSA	60	40

of polymer film was kept in the solvent mixture (50:50) of xylene and dimethylformamide (DMF) at room temperature for 24 h, followed by drying of the film at 80 °C until a constant weight was achieved. The gel content of the cured film was then determined by the formula:

$$\text{Gel content } (\%) = \frac{\text{Weight of the coating after 24 h of solvent immersion}}{\text{Initial weight of the coating}} \times 100. \quad (2)$$

ASTM D570 was used to determine the water absorption of the cured coating film, in which the film was weighed before soaking in the water for 24 h. After 24 h, the film was removed from the water and dried with a paper towel to achieve a constant weight. Water absorption was determined from the differences in the weight of samples before and after soaking in the water according to the following equation:

$$\text{Water absorption } (\%) = \frac{(Wf - Wi)}{Wi} \times 100, \quad (3)$$

where *Wi* and *Wf* are the initial weight of the coating before water absorption test and final weight of the coating after water absorption test, respectively.

The chemical structures of PA and PSA were identified by Fourier transform infrared (FTIR) spectroscopy on a Bruker ATR spectrophotometer, USA. The spectra were observed in the range of 600–4000 cm^{-1} wavenumbers. The structure confirmation of PA and PSA was done by ^{1}H, ^{13}C and ^{31}P nuclear magnetic resonance (NMR) spectroscopy. NMR spectra of the product were analyzed using a Bruker DPX 800 MHz spectrophotometer with dimethyl sulfoxide (DMSO) as a solvent.

Thermogravimetric analysis (TGA) of cured epoxy films was conducted on a PerkinElmer TGA 4000 instrument under the nitrogen atmosphere. Thermal analysis was monitored in the temperature range of 40–600 °C with 20 °C/min heating rate. Differential scanning calorimetry (DSC) (TA Q100 analyzer, USA) was employed for determination of the glass transition temperature (T_g) of cured films. The film sample was weighed accurately in an aluminum pan

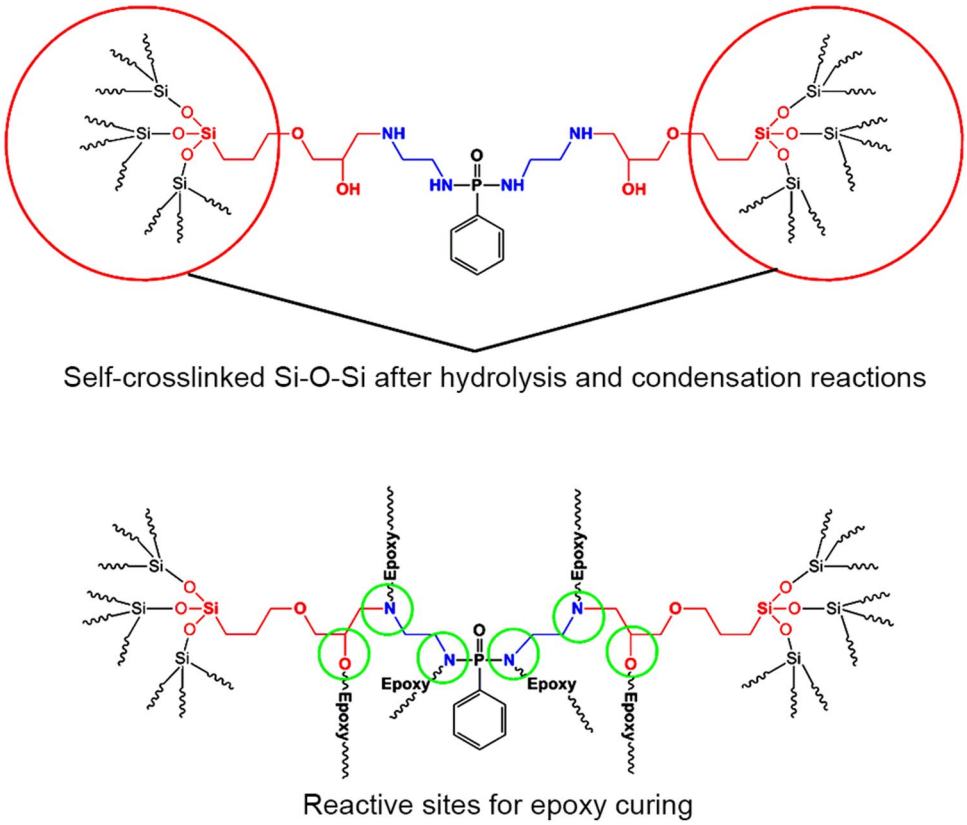

Fig. 2 Schematic diagram showing the hydrolysis and condensation reactions of methoxy groups of the silane and curing of epoxy resin with PSA

and heated in 40–120 °C temperature range with a heating rate of 10 °C/min.

The coatings were characterized by performing various mechanical tests according to ASTM standards. The adhesion of the coating onto the substrate was examined by the crosscut test according to ASTM D-3359. On the coating surface, a lattice marking of 1 cm^2 was done until the metal surface was exposed, followed by the application of adhesion tape over lattice marking. The adhesive tape was then pulled out from the coating surface, and adhesion failure was examined over the lattice marking as per ASTM standard. Pencil hardness test was carried out according to the ASTM D-3363. Scratch was made on the coating surface using 6B–6H range of pencils at an angle of 45°. The impact properties of the coatings were evaluated by dropping a weighed ball of 1.36 kg from the maximum height of 60 cm onto the coated surface. The flexibility of the coatings was evaluated using a conical mandrel as per ASTM D-522. The coated panels were fixed onto a conical mandrel and were bent to analyze the coating flexibility.

The flammability of the cured samples was investigated by limiting oxygen index (LOI) test carried out on Dynisco, USA, according to ASTM D2863 procedure. The UL-94 vertical burning test was carried out according to ASTM D1356-2005. Sample specimens having a size of $125 \times 12.5 \times 3$ mm were mounted vertically, and the flame was introduced for 10 s to the specimen at an angle of 45°. The detailed rating is given in Table 2.

Results and discussion

Physicochemical analysis

Both the synthesis reactions of PA and PSA were monitored by calculating the amine values which are then compared

Table 2 UL-94 rating

Rating	Description
V-0	Burning stops within 10 s on a vertical specimen; drips of particles allowed as long as they are not inflamed.
V-1	Burning stops within 30 s on a vertical specimen; drips of particles allowed as long as they are not inflamed.
V-2	Burning stops within 30 s on a vertical specimen; drips of flaming particles are allowed.

Table 3 Physicochemical analysis of PA and PSA

Sample	Experimental amine value (mg KOH/g resin)	Theoretical amine value (mg KOH/g resin)
PA	919.4	926.3
PSA	308.5	313.9

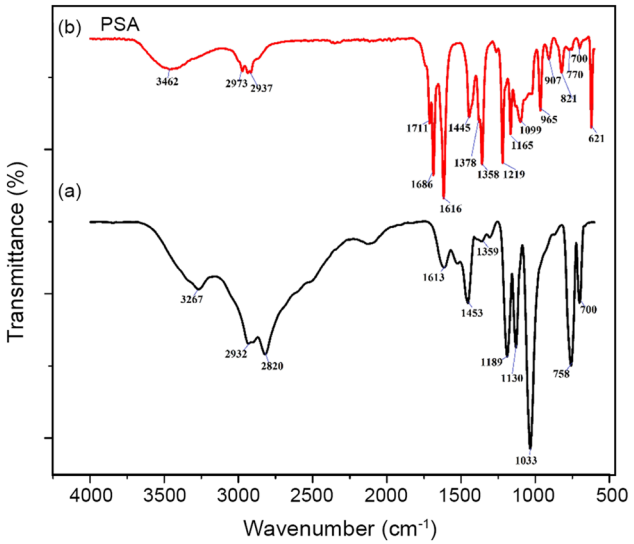

Fig. 3 FTIR spectra of PA and PSA

with theoretical values and depicted in Table 3. The results revealed that the obtained amine values are comparable and the desired structures might have formed.

FTIR and NMR analysis

The FTIR spectra of the PA are given in Fig. 3a. The bands at 3267 cm^{-1} are attributed to N–H stretch, suggesting the presence of the amines in the compound. The bands at 2932 and 2820 cm^{-1} correspond to the C–H stretch, indicating the presence of aliphatic chains in the system. The band at 1613 cm^{-1} corresponds to N–H bend for primary amines. The peak at 1453 cm^{-1} corresponds to the C–C stretch (in the ring), showing the presence of the aromatic ring. The peak at 1189 cm^{-1} is attributed to P=O stretch, and the peak at 1033 cm^{-1} indicates the presence of P–N–C stretch, confirming the completion of the reaction. The FTIR spectra of the PSA are shown in Fig. 3b. The band at 3462 cm^{-1} is attributed to the O–H stretching vibration. The peak at 2973 cm^{-1} is assigned to the presence of O–CH_3 stretching vibration, and the peak at 2937 cm^{-1} is assigned to the presence of O–CH_2 stretching vibration. The peak at 1616 cm^{-1} corresponds to N–H bend for primary amines. The peak at 1445 cm^{-1} corresponds to C–C stretch in the aromatic ring. The peak at 1378 cm^{-1} indicates the presence of CH–OH secondary free alcohol. The peak at 1358 cm^{-1} corresponds to C–H bend vibrations. The peak at 1219 cm^{-1} corresponds to the C–N stretching vibrations. The peak at 1165 cm^{-1} corresponds to P=O stretch. The band at 1099 cm^{-1} corresponds to the P–N–C stretch, suggesting the presence of the PA compound. The peak at 965 cm^{-1} corresponds to Si–O–C stretching vibrations, and the peak at 907 cm^{-1} gives the Si–O stretching vibration.

The ^{1}H, ^{13}C and ^{31}P NMR spectra of PSA are shown in Fig. 4a–c, respectively. The ^{1}H NMR spectrum shows the peak in the region of 7.15–7.45 ppm due to the AR–H protons. The peak at 3.08 ppm is due to the presence of O–H proton. The peak at 3.18–3.28 ppm shows the presence of O–CH_3 protons in the silicon compound. The peaks around 1.03 ppm and 0.55–0.62 ppm are due to –NH_2 protons. The ^{13}C NMR spectrum shows all the aromatic carbons in the range of 127.63–131.45 ppm. The carbon attached to O atom and N atom appeared in the range of 50.84–70.18 ppm. The ^{31}P NMR spectrum shown in Fig. 4c shows a characteristic peak at 27.41 ppm which is due to the presence of phosphorus. From all the data obtained, it is confirmed that the desired product is formed.

Thermal properties

TGA of the cured samples was done to study the changes in physical and chemical properties of the agent. The TGA curves of the various samples are shown in Fig. 5, and the characteristic thermal behavior of the cured samples is shown in Table 4. The initial degradation temperatures of the polymeric matrices are dependent on the volatile matter and the initial chain relaxations due to the thermal energy. Although there is incorporation of thermally stable atoms, the bulky nature of the PSA is needed to be considered. The bulky nature of the PSA causes faster chain relaxation because of the increased voids and decreased packing density throughout the polymer matrix which leads to early degradation of polymer chains [3, 14]. The initial degradation of the polymeric networks did not follow any trend which can be attributed to the competency of the decreased packing density because of the bulky nature of the PSA and simultaneous incorporation of the thermally stable P and Si atoms. However, the char yield at 700 °C increases with an increase in the concentration of the curing phosphorus content, and not only the thermal stability of the material increases but also its decomposition increases by char formation which prevents further decomposition of the epoxy backbone. The residual char formation acts as a barrier against fire by reducing thermal conductivity and thereby resisting the heat transfer from the flame to the material. This helps in preventing the further decomposition of the material [15]. The results explain that P- and Si-containing compounds

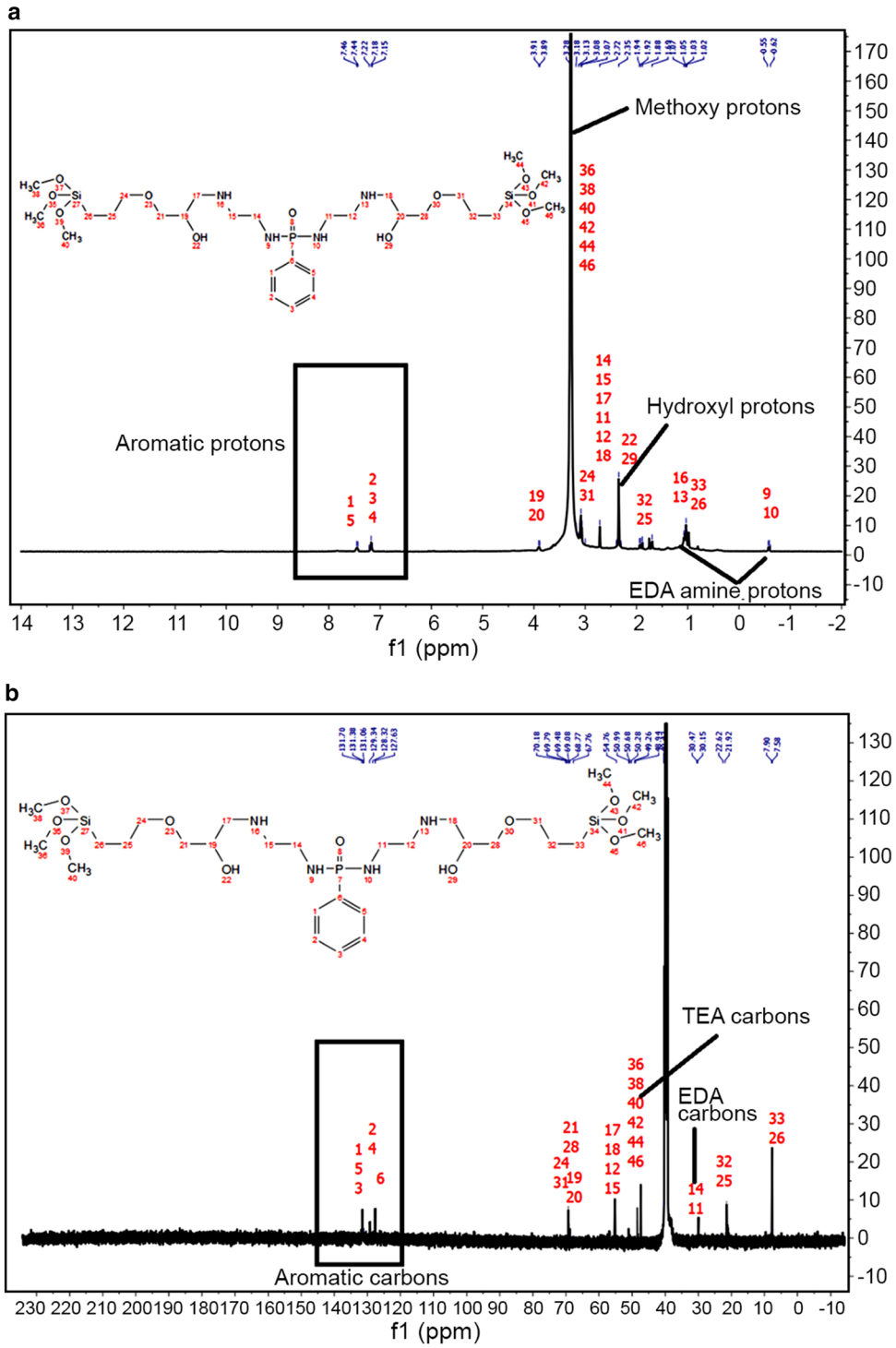

Fig. 4 **a** ^{1}H NMR spectra of PSA, **b** ^{13}C NMR spectra of PSA and **c** ^{31}P NMR spectra of PSA

show synergistic effects in the condensed phase, where P plays an important role in char formation and Si promotes it as well [16]. The heat resistance index temperature (T_{HRI}) is calculated using the following formula and it is presented in Table 4.

$$T_{HRI} = 0.49 \times [T5 + 0.6 \times (T30 - T5)]$$

The data show that the thermal stability of the coatings reflects the effect of an irregular trend in initial degradation behavior of the coatings [17–19].

Fig. 4 (continued)

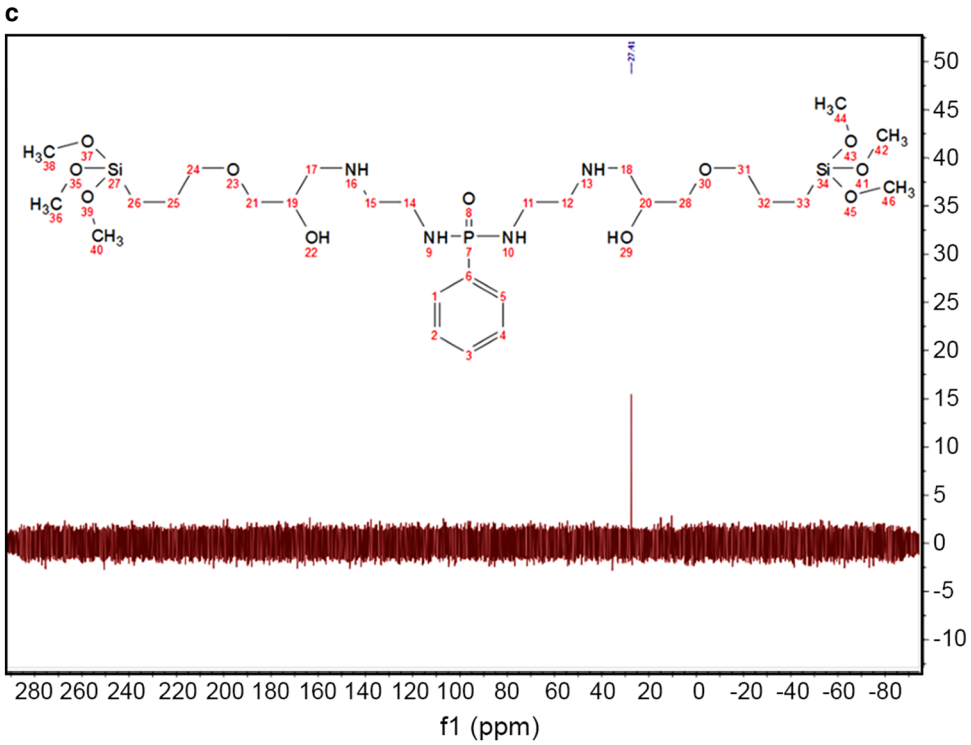

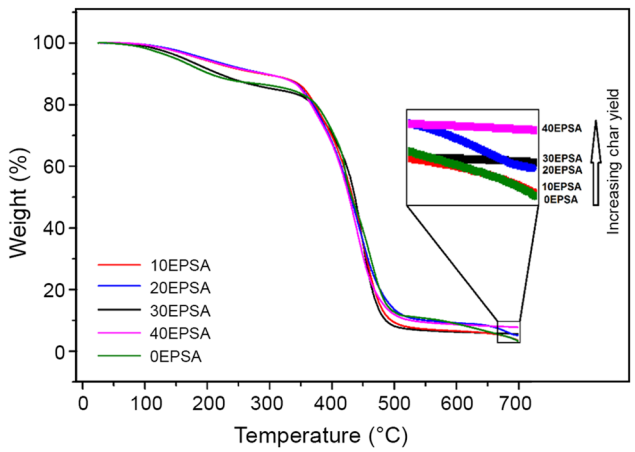

Fig. 5 TGA curves of EPSA coatings

Table 4 Thermal properties of cured epoxy resins

Sample	T_g (°C)	5% weight loss [T5] (°C)	30% weight loss [T30] (°C)	T_{HRI} (°C)	% Residue at 700°C
0EPSA	71.4	187.3	399.3	154.1	3.36
10EPSA	72.2	149.1	404.0	147.9	3.38
20EPSA	78.5	195.9	395.3	154.6	5.16
30EPSA	80.5	162.4	401.2	149.7	5.53
40EPSA	81.2	189.0	393.3	152.6	7.73

The glass transition temperature (T_g) values of the epoxy cured samples are given in Table 4, and DSC curves are shown in Fig. 6. The results indicate that the T_g values of the cured samples increase as the concentration of the curing agent increases. This is due to the presence of a phenylene ring which is attached to the phosphorus, due to which intermolecular distance increases and the motion of the molecule is hindered, and it results in the formation of high T_g [20, 21]. Incorporation of P and Si leads to an increase in T_g due to the presence of a bulky group in the backbone of the curing agent. The increase in the crosslinking density of the molecule may be another factor that affects the T_g of the system [22, 23].

Mechanical properties

The various mechanical properties of the coatings such as pencil hardness, flexibility and crosscut test were performed to determine the ability of the coating to resist stress. The results showed that the properties of the coatings are improved by increasing the content of PSA curing agent. This may be attributed to the crosslinked structure which gives rise to certain properties [24]. The mechanical properties of the coating are shown in Table 5. The EPSA 40% showed pencil hardness above 4H as compared with the coating containing only commercial epoxy and polyamide. The coating properties were also evaluated by the crosscut test. All the coatings showed 100% adhesion to the metal

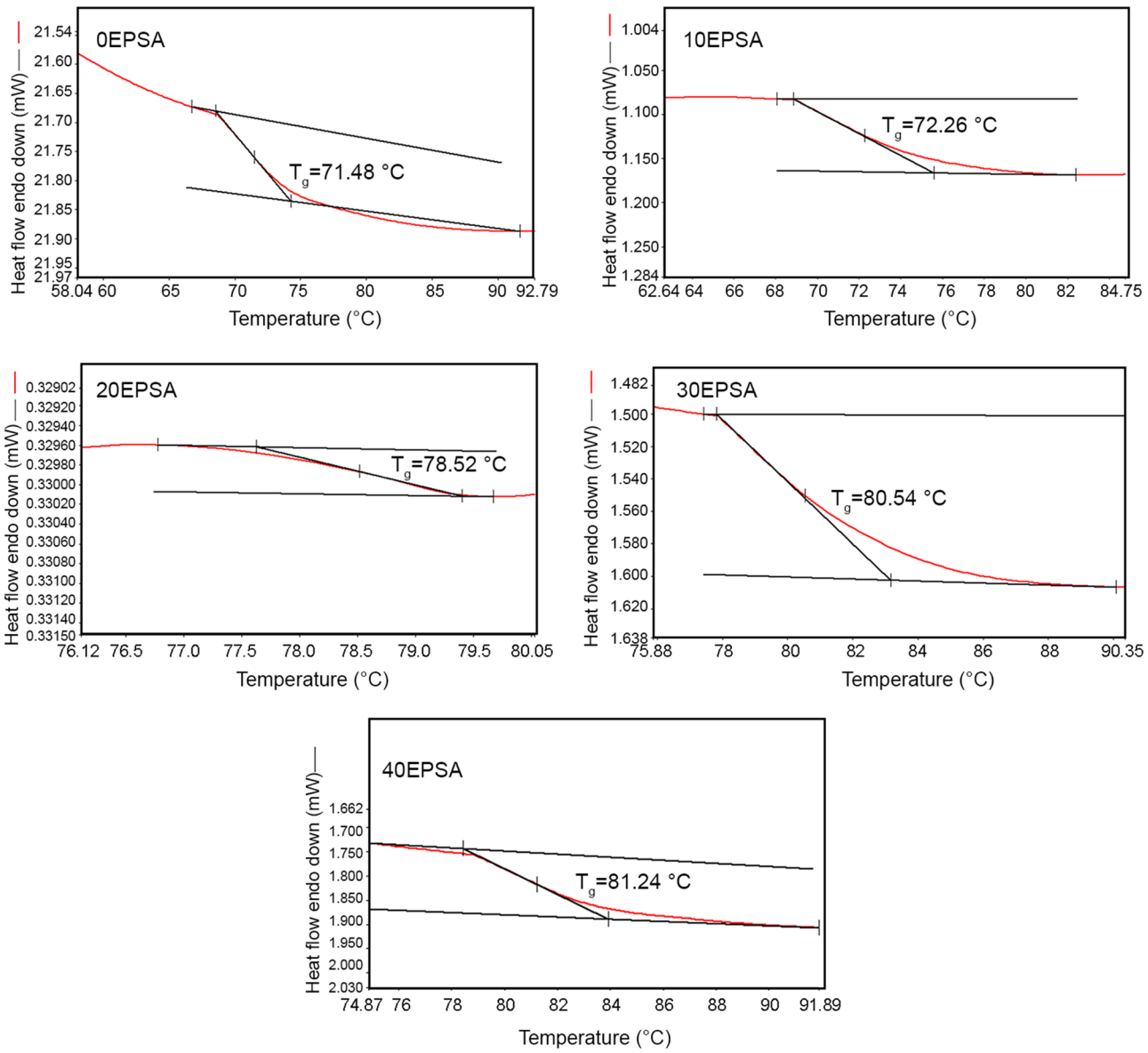

Fig. 6 DSC thermograms of EPSA coatings

substrate which is due to the presence of polar groups in the structure and hydrogen bonding with the metal substrate. Furthermore, the flexibility of the coatings is observed to be excellent without any crack in the coatings. This is due to the presence of aliphatic chains in the structure which attribute flexibility to the system and the polar groups which create strong molecular bonding [25]. The impact properties of all the coatings have found to be good. This may be attributed to the proper balance maintained between the soft and hard segments of the resin (Table 5).

The gloss of the coating samples is shown in Fig. 7. The gloss of the coatings decreases with an increase in the concentration of FR curing agent. The effect of P and Si on the surface smoothness properties was determined by the gloss test at 60° angle.

The gel content (Fig. 8) of the cured samples was evaluated in the solvent mixture of xylene and DMF for 24 h. The gel content of the samples increased with an increase in PSA concentration. The crosslinking density governed the gel content of the samples which reflected in an increasing trend due to the self-crosslinking of PSA over hydrolysis and condensation and the crosslinking due to epoxy and PSA structure of GPTMS which resulted in improper stacking of the polymer chains [24]. However, the gel content is also often correlated to the hydrophobicity, i.e., the barrier property of the material, and here, the incorporation of Si in

Table 5 Mechanical properties of cured epoxy coatings

Sample	Impact test (cm)	Flexibility	Solvent scrub test (rubs)	Pencil hardness	Crosscut test
0EPSA	55	0.1 mm	> 450	2H	Pass
10EPSA	60	0 mm		4H	
20EPSA					
30EPSA				5H	
40EPSA					

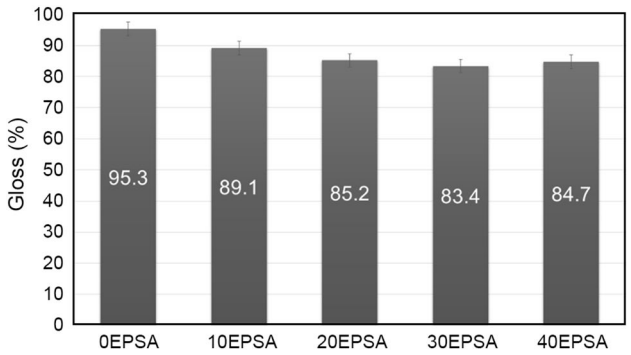

Fig. 7 Gloss of EPSA coatings

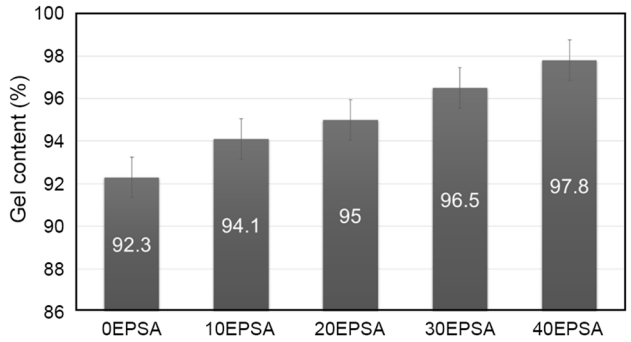

Fig. 8 Gel content of EPSA coatings

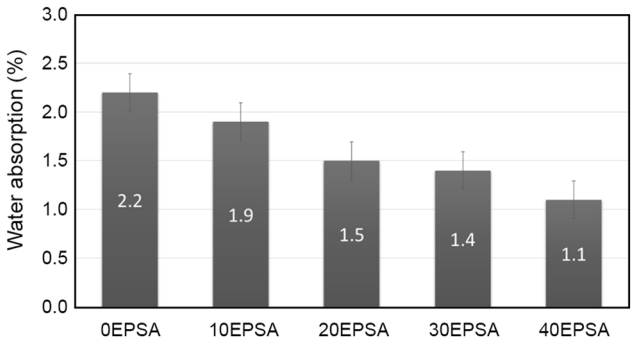

Fig. 9 Water absorption of EPSA coatings

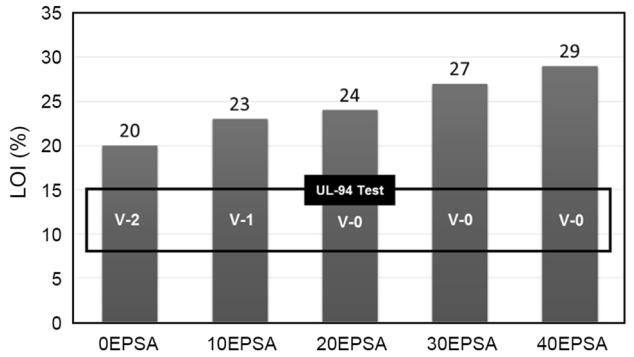

Fig. 10 LOI and UL-94 vertical burning test results of EPSA coatings

the system has increased the hydrophobicity of the coating material, and hence, 40EPSA shows the highest gel content.

The cured samples were immersed in water for 24 h to determine the percentage of water migrated in cured coatings. Figure 9 shows the results of the water absorption test. This property is obviously governed by the crosslinking density of the material, i.e., the higher the crosslinking density, the lower will be the water absorption. Hence, 40EPSA shows the lowest water absorption because of the combined effect of crosslinking density and incorporation of Si in the coating system [26–28].

The solvent scrub resistance test was carried out by rubbing the samples for over 450 cycles by using MEK and xylene. The results (Table 5) revealed that the cured samples were sufficiently crosslinked which prevented any defects like the dissolution of film or loss of gloss. The high resistance to solvent scrub is due to the highly crosslinked structure of the cured films and the presence of N–H groups which create a hydrogen bonding in it or with other molecules or substrate [8, 29].

FR properties

FR properties of the coatings were evaluated by performing the LOI test, and the obtained results are shown in Fig. 10 which indicates that the LOI values of the coatings increase as the concentration of phosphorus and silicon increases. LOI values significantly increased from 20 to 29 as the phosphorus and silicon concentrations were increased in the epoxy resin. The highest LOI value of 29 is associated with a

coating containing 40% concentration of curing agent, which may be due to the char enrichment of phosphorus and char promoting effect of silicon, i.e., the synergistic effect of both atoms [8, 20]. The phosphorus compound during combustion at elevated temperature is converted into phosphoric acid and water. The phosphoric acid undergoes further reaction forming an inorganic polymeric layer, suppressing the combustion of the coating protecting the base substrate, whereas the water helps in lowering the temperature of the coating [29]. The silicon atom itself is known for its inherent thermal stability at elevated temperatures; the incorporation of the same into the coating formulations increases the inherent thermal stability of the polymer backbone. Furthermore, it has been reported that the phosphorus-containing compounds reduce the flammability of the polymer matrices through their radical scavenging mechanisms in the gas phase which are responsible for the combustion (e.g., $^{\bullet}$H, $^{\bullet}$OH).

The burning behavior of the coatings was characterized by performing the UL-94 vertical burning test. All coating samples showed self-extinguishing behavior except the coatings with 0% and 10% content of curing agent. The coatings exhibiting self-extinguishing behavior were able to quench the fire within a period of 5–10 s when the flame was removed. The burning residue of the coatings with the minimum concentration of curing agent did fall off, while 20EPSA, 30EPSA and 40EPSA did not produce any dripping.

Conclusion

Phosphorus- and silicon-containing FR curing agent for epoxy resin has been synthesized successfully. The incorporation of P and Si into epoxy resin led to increased flame retardancy as well as the thermal stability of the material. Among the cured samples, the sample with 40% content of P and Si flame retardant curing agent showed the best FR properties with the char yield of 7.732% and the LOI of 29. All samples with PSA possess high glass transition temperature, improved structural stability and good mechanical properties than commercial epoxy and polyamide system. This curing agent can be used along with the various commercial epoxy resins; also one can use different polyamines in the first step to obtain the desired properties.

References

1. Agrawal S, Narula AK (2014) Synthesis and characterization of phosphorus and silicon containing flame-retardant curing agents and a study of their effect on thermal properties of epoxy resins. J Coat Technol Res 11:631–637
2. Patel M, Mestry S, Phalak G, Mhaske S (2019) Novel catechol-derived phosphorus-based precursors for coating applications. Polym Bull 60:229–236
3. Szolnoki B, Toldy A, Konrad P, Szebenyi G, Marosi G (2013) Comparison of additive and reactive phosphorus-based flame retardants in epoxy resins. Period Polytech Chem Eng 2:85–91
4. Patil DM, Phalak GA, Mhaske ST (2019) Novel phosphorus-containing epoxy resin from renewable resource for flame-retardant coating applications. J Coat Technol Res 16:531–542
5. Gu J, Dang J, Wu Y, Xie C, Han Y (2012) Flame-retardant, thermal, mechanical and dielectric properties of structural non-halogenated epoxy resin composites. Polym-Plast Technol 51:1198–1203
6. Liu W, Wang Z, Xiong L, Zhao L (2010) Phosphorus-containing liquid cycloaliphatic epoxy resins for reworkable environment-friendly electronic packaging materials. Polymer 51:4776–4783
7. Levchik SV, Weil ED (2004) Thermal decomposition, combustion and flame-retardancy of epoxy resins: a review of the recent literature. Polym Int 53:1901–1929
8. Mestry S, Kakatkar R, Mhaske ST (2019) Cardanol derived P and Si based precursors to develop flame retardant PU coating. Prog Org Coat 129:59–68
9. Shia Y, Wang G (2016) The novel silicon-containing epoxy/PEPA phosphate flame retardant for transparent intumescent fire-resistant coating. Appl Surf Sci 385:453–463
10. Zhang W, Li X, Yang R (2011) Pyrolysis and fire behavior of epoxy resin composites based on a phosphorus-containing polyhedral oligomeric silsesquioxane (DOPO-POSS). Polym Degrad Stab 96:1821–1832
11. Li C, Fan H, Hu J, Li B (2012) Novel silicone aliphatic amine curing agent for epoxy resin: 1,3-Bis (2-aminoethylaminomethyl) tetramethyldisiloxane. 2. Isothermal cure, and dynamic mechanical property. Thermochim Acta 549:132–139
12. Ménard R, Negrell C, Fache M, Ferry L, Sonnier R, David G (2015) From a bio-based phosphorus-containing epoxy monomer to fully bio-based flame-retardant thermosets. RSC Adv 5:70856–70867
13. Lin Y, Sun J, Zhao Q, Zhou Q (2012) Synthesis and properties of a novel flame-retardant epoxy resin containing biphenylyl/phenyl phosphonic moieties. Polym Plast Technol 51:896–903
14. Wang Y, Yuan Y, Zhao Y, Liu S, Zhao J (2016) Flame–retarded epoxy resin with high glass transition temperature cured by DOPO-containing H-benzimidazole. High Perform Polym 29:94–103
15. Rao WH, Liao W, Wang H, Zhao HB, Wang YZ (2018) Flame-retardant and smoke-suppressant flexible polyurethane foams based on reactive phosphorus-containing polyol and expandable graphite. J Hazard Mater 360:651–660
16. Qi J, Wen Q, Zhu J (2019) Synergistic effect of intumescent flame retardant system consisting of hexophenoxy cyclotriphosphazene and ammonium polyphosphate on methyl ethyl silicone rubber. Mater Lett 249:62–65
17. Guo Y, Lyu Z, Yang X, Lu Y, Ruan K, Wu Y, Kong J, Gu J (2019) Enhanced thermal conductivities and decreased thermal resistances of functionalized boron nitride/polyimide composites. Compos B-Eng 164:732–739
18. Gu J, Lv Z, Wu Y, Guo Y, Tian L, Qiu H, Li W, Zhang Q (2017) Dielectric thermally conductive boron nitride/polyimide composites with outstanding thermal stabilities via in situ polymerization electrospinning-hot press method. Compos Part A Appl S 94:209–216
19. Tang L, Dang J, He M, Li J, Kong J, Tang Y, Gu J (2019) Preparation and properties of cyanate-based wave-trans- parent laminated composites reinforced by dopamine/POSS functionalized kevlar cloth. Compos Sci Technol 169:120–126

20. Quin LJ, Ye LJ, Xu GZ, Liu J, Guo JQ (2011) The nonhalogen flame retardant epoxy resin based on a novel compound with phosphaphenanthrene and cyclotriphosphazene double functional groups. Polym Degrad Stab 96:1118–1124
21. Qian L, Zhi J, Tong B, Jianbing S, Fan Y, Yuping D (2009) Synthesis and characterization of main chain liquid crystalline copolymers containing phosphaphenanthrene side-groups. Polymer 50:4813–4820
22. Sag J, Goedderz D, Kukla P, Greiner L, Schönberger F, Döring M (2019) Phosphorus-containing flame retardants from biobased chemicals and their application in polyesters and epoxy resins. Molecules 24:1–31
23. Wu CS, Liu YL, Chiu YS (2002) Epoxy resins possessing flame retardant elements from silicon incorporated compounds cured with phosphorus or nitrogen containing curing agents. Polymer 43:4277–4284
24. Mestry S, Mhaske ST (2019) Synthesis of epoxy resins using phosphorus-based precursors for flame-retardant coating. J Coat Technol Res 16:807–818
25. Choia JS, Seob J, Khanc SB, Janga ES, Han H (2011) Effect of acrylic acid on the physical properties of UV-cured poly(urethane acrylate-co-acrylic acid) films for metal coating. Prog Org Coat 71:110–116
26. Manfredi LB, Fraga AN, Vazquez A (2006) Influence of the network structure and void content on hygrothermal stability of resol resin modified with epoxy-amine. J Appl Polym Sci 102:588–597
27. Saijun D, Nakason C, Kaesaman A, Klinpituksa P (2009) Water absorption and mechanical properties of water-swellable natural rubber. Songklanakarin J Sci Technol 31:561–565
28. Huang ZG, Shi WF (2007) Synthesis and properties of a novel hyperbranched polyphosphate acrylate applied to uv curable flame retardant coatings. Eur Polym J 43:1302–1312
29. Wang X, Hu Y, Song L, Xing W, Lu H (2010) Thermal degradation behaviors of epoxy resins/POSS hybrids and phosphorus–silicon synergism of flame retardancy. J Polym Sci 48:693–705